Int J Adv Manuf Technol (2012) 60:545–552
DOI 10.1007/s00170-011-3630-x

ORIGINAL ARTICLE

Study on the generative design method and error budget of a novel desktop multi-axis laser machine for micro tool fabrications

Xiang Cheng · Yumei Huang · Shuangjie Zhou · Junying Liu · Xianhai Yang

Received: 27 March 2011 / Accepted: 9 September 2011 / Published online: 23 September 2011

Abstract Micro end mills made of hard or ultra-hard materials are mainly fabricated by grinding or by wire electrical discharge machining (WEDM). However, with the advances of new tool materials from ultra-hard to super-hard together with lower or no electrical conductivity such as the material of nano-polycrystalline diamond, the grinding or the WEDM method cannot be used for machining due to their ultra-low process efficiencies for such materials. Laser machining has been tested an effective method. Accordingly, multi-axis laser machines need to be designed for micro tool fabrications. In the paper, a typical micro ball end mill with relatively complex features has been analyzed by the generative design method to generate the number and properties of needed motion axes. Based on the analysis, a novel five-axis laser machine has been designed. Aiming at high-quality micro tool fabrications, the kinematics model has been derived for this five-axis laser machine and error budge has been studied for the subsequently optimum selection of key motion components.

X. Cheng (✉) · J. Liu · X. Yang
Shandong Provincial Key Laboratory of Precision Manufacturing and Non-traditional Machining,
Shandong University of Technology,
Zibo 255049, China
e-mail: cxcheng@ucdavis.edu

Y. Huang
School of Mechanical Instrumental Engineering,
Xi'an University of Technology,
Xi'an 710048, China

S. Zhou
Nantong Ya Hua Shipbuilding Group Co., Ltd,
Nantong, Jiangsu 226361, China

Keywords Micro tool · Generative design method · Error budget · Laser machine

1 Introduction

Mechanical micro/nano machining is gaining more and more importance due to the miniaturization tendency of products throughout the world. However, micro/nano machining process is performed under lower feed rates and smaller depths of cut comparing with conventional machining, which results in comparatively longer micromachining time. Consequently, longer tool life is needed. Ultra-hard materials such as cubic boron nitride (CBN) and polycrystalline diamond (PCD) are usually selected as tool materials to fulfill this requirement. To fabricate micro tools made of CBN or PCD, the grinding method is usually applied commercially and the wire electrical discharge machining (WEDM) method is also successfully applied in custom micro tooling [1, 2].

With the advances of new technologies, NPD is a new material made directly from graphite by direct conversion under high temperature and high pressure. It has the Knoop hardness of 120–145 GPa, which is higher than those of natural single crystal diamond [3, 4]. Therefore, it is an ideal material for micro tooling. Recently, micro ball end mills have been created [4]. However, by the grinding method using the soft materials to grind the hard materials, the machining efficiency is very low.

The WEDM uses a thin single-strand metal wire as the electrode to cut through the workpiece, which is one of the most favorable variants owing to its ability to machine conductive, exotic, and high-strength and temperature-resistive (HSTR) materials with the scope of generating intricate shapes and profiles [5]. Also, spools of wire are

typically very long. For example, a 5-kg spool of 0.1-mm-diameter wire is just over 20 km long and it can cut for about 60 h, which makes the batch production possible. An appropriate manufacturing process to cover the growing need for accurate small tools is EDM with thin wires [6]. WEDM has been gaining wide acceptance in the machining of the various materials used in modern tooling applications [7]. However, the ultra-hard nano-polycrystalline diamond is electrically nonconductive, which makes it impossible or very difficult to machine the material by WEDM method.

According to literature [8], laser machining techniques seems a good choice. Consequently, laser machine tools are needed for the fabrication of micro tools. There is limited research on the special purpose laser machines made for the fabrication of micro/nano milling tools. Also such kind of special purpose laser machine does not exist in the market yet. Furthermore, desktop or mesoscale machine tools are getting more and more importance for their inherent attributes [9, 10]. This paper attempts to give a basic study from the functional design point of view for a desktop machine tool.

Like any design, it is critical that the best concept is chosen in the early stage of the design process because 80% of the final cost and quality of a product are designed at this phase [11], which can also be applied to machine tool design. A generative design method was introduced in [12] and used for a lathe design, which gave reasonable and intuitionistic answers to machine tool designs. By this method, a six-axis WEDM machine has been functionally analyzed and developed [13, 14].

In this paper, the generative design method is studied and expanded to the function design of the multi-axis laser machine for the fabrication of micro tools. First, the geometry features, namely the generating line and guide line, of the typical ball end mill are defined. Second, the mathematical model to describe the interrelation between the tool blank geometry and the laser focal point is derived. Based on the mathematical model, the required number of the axes and axis motions are obtained. According to the characteristics of specialized laser machine, the schematic three dimensional CAD models are created. In order to acquire a high-accuracy laser machine, the kinematics model is built and consequent error budget has been made to guide the optimum selection of the motion components in the future.

2 Generative kinematics design

2.1 Typical geometric analysis

In mechanical micro/nano machining, micro tools used in micro/nano milling is comparatively more complicated in geometry than that used in micro/nano turning, shaping, etc. Therefore, in this paper, a micro ball end mill is selected for analysis as it has the near freeform geometries. The selected micro ball end mill pictures and CAD models are shown in Fig. 1.

The geometric model of the selected ball end mill is shown in Fig. 2, where the most important geometrical features, namely the cutting edge and rake and clearance faces, are depicted. O is the center of the ball shape, circle ACA is the cross section of the ball at the middle with the center O, arc ABC is the cutting edge, P is an arbitrary point on the cutting edge with the central angle of β, R is the radius of the ball shape, the half circle $A_1B_1C_1$ is auxiliary for the following analysis, the plane $A_1B_1C_1$ is parallel to the cutting edge plane ABC with the distance of L, O_1 is the center of arc $A_1B_1C_1$, P_1 is the corresponding point on arc $A_1B_1C_1$ to point P with the same central angle of β, α is the absolute value of the rake angle. To form the cutting edge and the rake and clearance faces, line AA_1 moves along the arc ABC and the arc $A_1B_1C_1$ respectively, which overlaps PP_1 while the central angel is β, overlaps BB_1 while β equals 90°and overlaps CC_1 while β equals 180°. The other half rake and clearance faces can be created with the same principle.

2.2 Generative design analysis

The coordinates are built as shown in Fig. 2, where $\sum O$ has the X-axis pointing from O to O_1, Y-axis pointing from O to A, and Z-axis is at the center line of the rotational axis of the ball end mill. $\sum P$ has the X-axis pointing from P to P_1, Y-axis pointing from O to P, and Z-axis is tangent to arc ABC at point P. Based on the generative design method as discussed in [13], line PP_1 is selected as the generating line, and arc ABC is selected as the guide line. Point P_1 represents the arbitrary point on the ball end mill geometry to be machined and overlaps P while L equals 0. According to the coordinates built above, the transformation matrix for the generating line can be written as,

$$ {}^{O}T_{P1} = \begin{bmatrix} 1 & 0 & 0 & 0 \\ 0 & C_\beta & -S_\beta & 0 \\ 0 & S_\beta & C_\beta & 0 \\ 0 & 0 & 0 & 1 \end{bmatrix} \begin{bmatrix} 1 & 0 & 0 & 0 \\ 0 & 1 & 0 & R \\ 0 & 0 & 1 & 0 \\ 0 & 0 & 0 & 1 \end{bmatrix} \begin{bmatrix} 1 & 0 & 0 & \frac{L}{S_\alpha} \\ 0 & 1 & 0 & 0 \\ 0 & 0 & 1 & 0 \\ 0 & 0 & 0 & 1 \end{bmatrix} \tag{1} $$

namely,

$$ {}^{O}T_{P1} = \begin{bmatrix} 1 & 0 & 0 & \frac{L}{S_\alpha} \\ 0 & C_\beta & -S_\beta & RC_\beta \\ 0 & S_\beta & C_\beta & RS_\beta \\ 0 & 0 & 0 & 1 \end{bmatrix} $$

where, C and S means the cosine function and sine function, respectively.

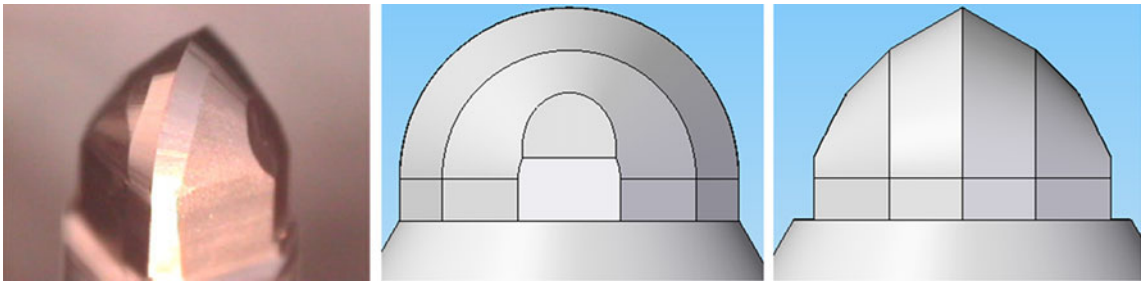

Fig. 1 Typical micro ball end mill [1, 2]

The transformation matrix for the guide line can be written as,

$$ {}^{O}T_{P} = \begin{bmatrix} 1 & 0 & 0 & 0 \\ 0 & C_\beta & -S_\beta & R \\ 0 & S_\beta & C_\beta & 0 \\ 0 & 0 & 0 & 1 \end{bmatrix} \tag{2} $$

The laser beam and its coordinate definition are shown in Fig. 3, where $\sum Q$ is the laser coordinate. Assume the focal point of the laser beam is a point for the convenience of analysis, P_3 is the focal point working as the cutter during micro tool fabrications and overlap P_1 on the micro tool. In practice, the focal radius will be taken into consideration as offset value. The transformation matrix for P_3 can be written as,

$$ {}^{Q}T_{P3} = \begin{bmatrix} 1 & 0 & 0 & 0 \\ 0 & 1 & 0 & 0 \\ 0 & 0 & 1 & d \\ 0 & 0 & 0 & 1 \end{bmatrix} \tag{3} $$

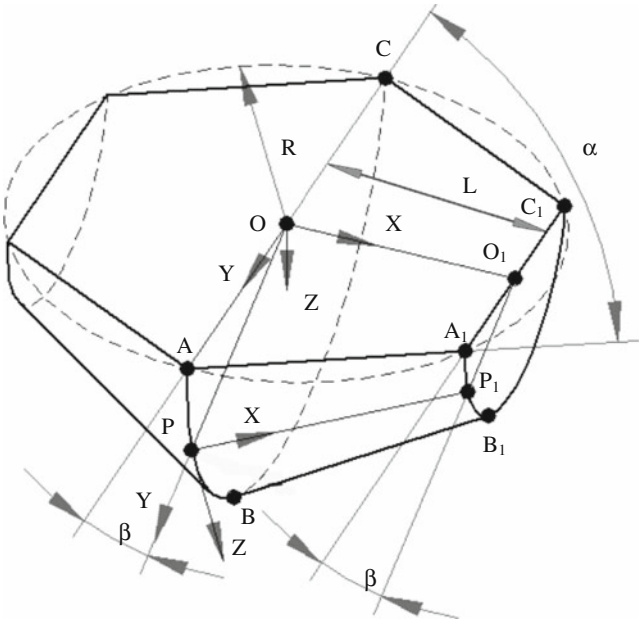

Fig. 2 Geometric model of the selected micro ball

From $\sum O$ to $\sum Q$ along the generating line and the guide line, the transformation matrices are Eqs. 4 and 5, respectively.

$$ {}^{O}T_{Q1} = \begin{bmatrix} 1 & 0 & 0 & \frac{L}{S_\alpha} \\ 0 & C_\beta & -S_\beta & RC_\beta + dS_\beta \\ 0 & S_\beta & C_\beta & RS_\beta - dC_\beta \\ 0 & 0 & 0 & 1 \end{bmatrix} \tag{4} $$

$$ {}^{O}T_{Q2} = \begin{bmatrix} 1 & 0 & 0 & 0 \\ 0 & C_\beta & -S_\beta & R + dS_\beta \\ 0 & S_\beta & C_\beta & -dC_\beta \\ 0 & 0 & 0 & 1 \end{bmatrix} \tag{5} $$

Based on the generative method, ${}^{O}T_{Q1}$ can be decomposed by T_{TX}, T_{TY}, T_{TZ}, and T_{RZ}, where T_{TX} and T_{RX} is the single-axis translational transformation matrix and rotational transformation matrix of axis X, respectively. Correspondingly, the kinematics representation of the motion axes can be written as $W/X\ Y\ Z\ \theta_Z/T$, where W and T represents the workpiece (micro tool) and tool (laser), respectively, the motions in the middle between the two "/" represents the single-axis motion combination to generate the generating line between the micro tool and laser. By the same method, ${}^{O}T_{Q2}$ can be decomposed by T_{TY}, T_{TZ}, and T_{RX}. The kinematics representation of the motion axes for generating the guide line can be written as $W/Y\ Z\ \theta_X/T$.

From above analysis, the total axes needed for the laser machine are five, namely, $W/X\ Y\ Z\ \theta_X\ \theta_Z$/T. From a safety point of view, the laser system is orientation fixed and the two rotational motions θ_X and θ_Z are assigned to the micro tool blank side. The micro tools have smaller geometrical sizes such as the diameter for micro milling tools is usually

Fig. 3 Coordinate of the laser beam

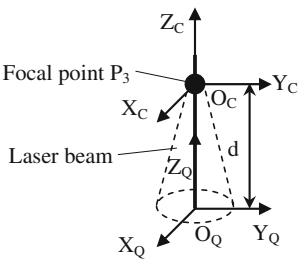

less than 1 mm. Therefore, the micro tool fabrication system by laser is to be designed as a desktop type as shown in Fig. 4. Considering the high accuracy needed for micro tool fabrications, granite material is used for the bed and main supporter. The laser system is fixed orientation pointing from top to the bed with *Z*-axis linear motion. The micro tool blank has two linear *X*- and *Y*-axis motions and two rotary *A* and *C*-axis motions.

3 Kinematics modeling

3.1 Forward kinematics

The coordinates are defined as shown in Fig. 5. To avoid confusions, coordinates other than the machine tool coordinate ΣO are marked only the origin points and they have the same orientations as that of the machine tool coordinate at their original state. ΣO_1, ΣO_2, ΣO_3, ΣO_4, and ΣO_5 represents the *X*-, *Y*-, *Z*-, *A*-, and *C*-axis coordinates, respectively.

The forward kinematics is to calculate the position and orientation of the micro tool blank and the focal point of the laser by given the motion variables of all motion axes. Assume the point being machined on the micro tool blank is P_W and focal point of the laser is P_L, the forward kinematics can be written as,

$$ {}^{O}T_{PW} = {}^{O}T_{O1}{}^{O1}T_{O2}{}^{O2}T_{O4}{}^{O4}T_{O5}{}^{O5}T_{PW} \tag{6} $$

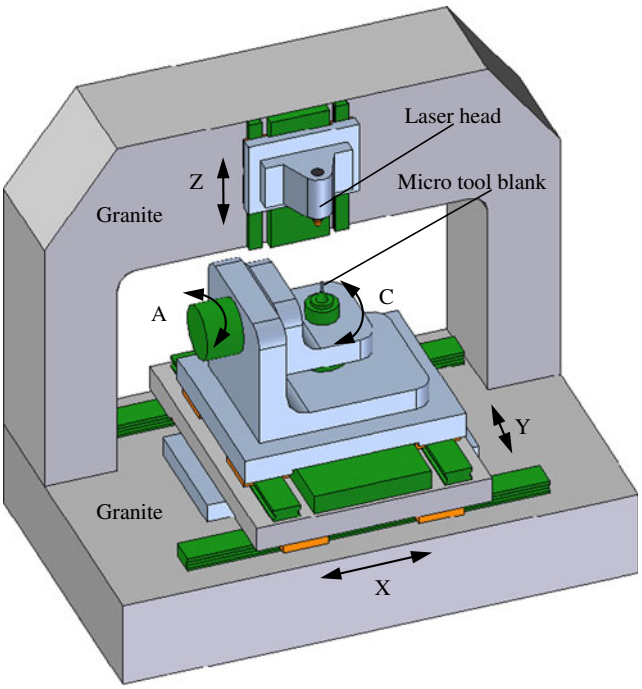

Fig. 4 Five-axis desktop laser machine

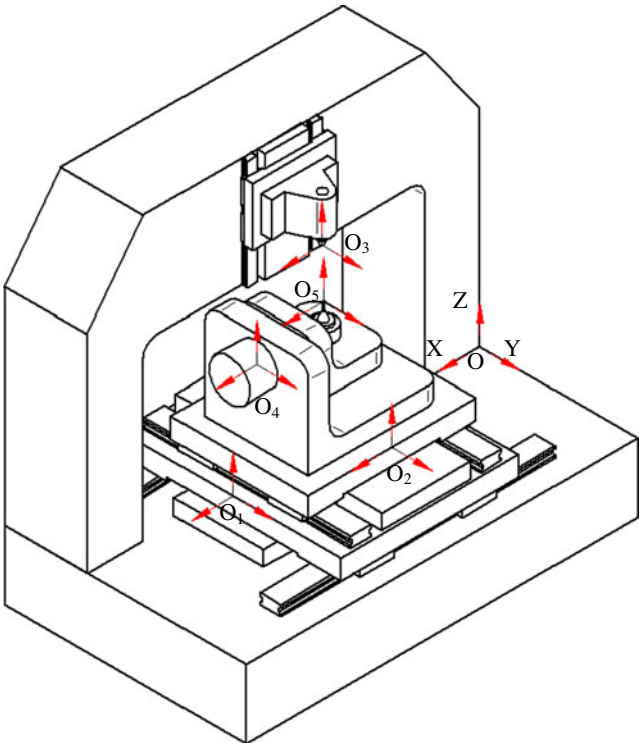

Fig. 5 Coordinates definition for the machine

$$ {}^{O}T_{PL} = {}^{O}T_{O3}{}^{O3}T_{PW} \tag{7} $$

where ${}^{R}T_{S}$ denotes the transformation matrix from coordinate ΣR to ΣS. For translational axes, the transformation matrix is relatively simple. Therefore, ${}^{O}T_{O4}$ can be derived directly as,

$$ {}^{O}T_{O4} = \begin{bmatrix} 1 & 0 & 0 & D_{X1}+X+D_{X2}+D_{X4} \\ 0 & 1 & 0 & D_{Y1}+D_{Y2}+Y+D_{Y4} \\ 0 & 0 & 1 & D_{Z1}+D_{Z2}+D_{Z4} \\ 0 & 0 & 0 & 1 \end{bmatrix} \tag{8} $$

where, D_{X1}, D_{X2}, D_{X4}, D_{Y1}, D_{Y2}, D_{Y4}, D_{Z1}, D_{Z2}, and D_{Z4} are the fixed structural parameters and can be calibrated after the machine is built. *X* and *Y* are *X*-axis and *Y*-axis linear motion variables, respectively.

$$ {}^{O4}T_{O5} = \begin{bmatrix} 1 & 0 & 0 & 0 \\ 0 & C_{\theta X} & -S_{\theta X} & 0 \\ 0 & S_{\theta X} & C_{\theta X} & 0 \\ 0 & 0 & 0 & 1 \end{bmatrix} \begin{bmatrix} 1 & 0 & 0 & D_{X5} \\ 0 & 1 & 0 & D_{Y5} \\ 0 & 0 & 1 & D_{Z5} \\ 0 & 0 & 0 & 1 \end{bmatrix} \tag{9} $$

$$ {}^{O5}T_{PW} = \begin{bmatrix} C_{\theta Z} & -S_{\theta Z} & 0 & 0 \\ S_{\theta Z} & C_{\theta Z} & 0 & 0 \\ 0 & 0 & 1 & 0 \\ 0 & 0 & 0 & 1 \end{bmatrix} \begin{bmatrix} 1 & 0 & 0 & D_{XW} \\ 0 & 1 & 0 & D_{YW} \\ 0 & 0 & 1 & D_{ZW} \\ 0 & 0 & 0 & 1 \end{bmatrix} \tag{10} $$

where, D_{X5}, D_{Y5}, and D_{Z5} are the fixed structural parameters and can be calibrated after the machine is built. D_{XW}, D_{YW}, and D_{ZW} are micro tool geometrical parameters and can be calculated when the micro tool geometry is fixed. θ_X and θ_Z are A-axis and C-axis rotational motion variables, respectively.

Correspondingly, the transformation matrix from ΣO to ΣO_{PW} is obtained as,

$$ {}^{O}T_{PW} = \begin{bmatrix} C_{\theta Z} & -S_{\theta Z} & 0 & D_1 + D_{XW}C_{\theta Z} - D_{YW}S_{\theta Z} + X \\ C_{\theta X}S_{\theta Z} & C_{\theta X}C_{\theta Z} & -S_{\theta X} & D_2 + D_{Y5}C_{\theta X} + D_{YW}C_{\theta X}C_{\theta Z} - D_3S_{\theta X} + D_{XW}C_{\theta X}S_{\theta Z} + Y \\ S_{\theta X}S_{\theta Z} & C_{\theta Z}S_{\theta X} & C_{\theta X} & D_4 + D_3C_{\theta X} + D_{Y5}S_{\theta X} + D_{YW}S_{\theta X}C_{\theta Z} + D_{XW}S_{\theta X}S_{\theta Z} \\ 0 & 0 & 0 & 1 \end{bmatrix} \tag{11} $$

where, $D_1=D_{X1}+D_{X2}+D_{X4}+D_{X5}$, $D_2=D_{Y1}+D_{Y2}+D_{Y4}$, $D_3=D_{Z5}+D_{ZW}$, $D_4=D_{Z1}+D_{Z2}+D_{Z4}$.

Transformation matrix from ΣO to ΣO_{PL} only includes linear motions, therefore ${}^{O}T_{\mathrm{PL}}$ can be obtained directly as,

$$ {}^{O}T_{PL} = \begin{bmatrix} 1 & 0 & 0 & D_{X3} \\ 0 & 1 & 0 & D_{Y3} \\ 0 & 0 & 1 & D_{Z3} + D_{FL} + Z \\ 0 & 0 & 0 & 1 \end{bmatrix} \tag{12} $$

where, D_{X3}, D_{Y3}, and D_{Z3} are the fixed parameters and can be calibrated after the machine is built. D_{FL} is the focal length of the laser and known when the laser source and lens are fixed. Z is the Z-axis linear motion variable.

3.2 Reverse kinematics

Reverse kinematics is to calculate the motion variables needed for motion axes by given the position and orientation requirements of the micro tool blank. Reverse kinematics model will be applied to the post processing process for generating CNC programs in a CAM system. Given the transformation matrix of ${}^{O}T_{\mathrm{PW}}$ as,

$$ {}^{O}T_{PW} = \begin{bmatrix} A_{11} & A_{12} & A_{13} & A_{14} \\ A_{21} & A_{22} & A_{23} & A_{24} \\ A_{31} & A_{32} & A_{33} & A_{34} \\ 0 & 0 & 0 & 1 \end{bmatrix} \tag{13} $$

From Eqs. 11 and 13, the five motion variables X, Y, Z, θ_X, and θ_Z can be solved for the purpose of control and post processing by CAM software.

4 Error budget analysis

Error budget analysis is to analyze the possible positioning errors each axis may contribute and to identify the optimum combinations of motion components with different accuracies to fulfill the given accuracy requirement. Based on the error budget, motion components can be selected conveniently at the design stage.

4.1 Error contribution analysis

For single motion axis, there are totally six errors. For example, the linear axis X has the straightness error in Y-axis and in Z-axis, roll error around X-axis, yaw error around Y-axis, pitch error around the Z-axis, and the positioning error in X-axis. The rotational C-axis has the radial error in X- and Y-axis, axial error in Z-axis, tilt error around X- and Y-axis, and the positioning error around Z-axis. The error budget will become ultra complicated if all these errors are considered. Furthermore, errors other than the positioning error for a single motion axis can be calibrated and compensated if they are repeatable. Therefore, in the paper, only the positioning errors for each axis are considered in order to simplify the analysis and to guide the motion component selection in the design stage.

Based on the forward kinematics, considering single-axis positioning errors, the positioning errors introduced from the motion axes are deduced [15].

$$ \begin{bmatrix} \Delta X_{PW} \\ \Delta Y_{PW} \\ \Delta Z_{PW} \end{bmatrix} = \begin{bmatrix} \Delta X + D_{XW}(C_{\theta_Z+\Delta\theta_Z} - C_{\theta_Z}) + D_{YW}(S_{\theta_Z+\Delta\theta_Z} - S_{\theta_Z}) \\ \Delta Y + \frac{1}{2}(B_1 + B_2 + B_3 + B_4 + B_5) \\ \frac{1}{2}(B_6 + B_7 + B_8 + B_9 + B_{10}) \end{bmatrix} \tag{14} $$

$$ \begin{bmatrix} \Delta X_{PL} \\ \Delta Y_{PL} \\ \Delta Z_{PL} \end{bmatrix} = \begin{bmatrix} 0 \\ 0 \\ \Delta Z \end{bmatrix} \tag{15} $$

where,

$$ \begin{aligned} B_1 &= 2D_{Y5}(C_{\theta_X+\Delta\theta_X} - C_{\theta_X}) \\ B_2 &= D_{YW}(C_{\theta_X+\Delta\theta_X-\theta_Z-\Delta\theta_Z} + C_{\theta_X+\Delta\theta_X+\theta_Z+\Delta\theta_Z} - C_{\theta_X+\theta_Z} - C_{\theta_X-\theta_Z}) \\ B_3 &= 2D_{Z5}(S_{\theta_X} - S_{\theta_X+\Delta\theta_X}) \\ B_4 &= 2D_{ZW}(S_{\theta_X} - S_{\theta_X+\Delta\theta_X}) \\ B_5 &= D_{XW}(S_{\theta_X+\Delta\theta_X+\theta_Z+\Delta\theta_Z} - S_{\theta_X+\Delta\theta_X-\theta_Z-\Delta\theta_Z} - S_{\theta_X+\theta_Z} + S_{\theta_X-\theta_Z}) \\ B_6 &= 2D_{Z5}(C_{\theta_X+\Delta\theta_X} - C_{\theta_X}) \\ B_7 &= 2D_{ZW}(C_{\theta_X+\Delta\theta_X} - C_{\theta_X}) \\ B_8 &= D_{XW}(C_{\theta_X+\Delta\theta_X-\theta_Z-\Delta\theta_Z} - C_{\theta_X+\Delta\theta_X+\theta_Z+\Delta\theta_Z} + C_{\theta_X+\theta_Z} - C_{\theta_X-\theta_Z}) \\ B_9 &= 2D_{Y5}(S_{\theta_X+\Delta\theta_X} - S_{\theta_X}) \\ B_{10} &= D_{YW}(S_{\theta_X+\Delta\theta_X-\theta_Z-\Delta\theta_Z} + S_{\theta_X+\Delta\theta_X+\theta_Z+\Delta\theta_Z} - S_{\theta_X+\theta_Z} - S_{\theta_X-\theta_Z}) \end{aligned} $$

ΔN is the N-axis positioning error.

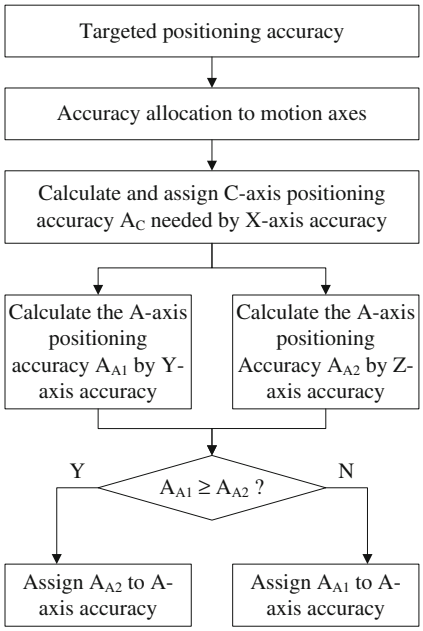

Fig. 6 Flow chart for the error budget

From the above equations, the key parameters are needed for the following analysis. The cutting edge diameter of micro tools is approximately smaller than 1 mm and the cutting edge length of the micro tools is smaller than 1 mm. Therefore, it is reasonable to set the following parameters as: D_{XW}=0.5 mm, D_{YW}=0.5 mm, D_{ZW}=5 mm. According the laser machine design, coordinates ΣO_4 and ΣO_5 have the same origin point in Y and Z axes. Correspondingly, D_{Z5}=D_{Y5}=0 mm. The stroke for A and C axes are 90° and 360°, respectively.

From Eqs. 14 and 15, the error contributions of three linear axes are only their positioning errors, while the positioning errors contributed by the two rotary axes are the functions combining the angular positions and angular positioning errors.

4.2 Error budget analysis

Error budget is to assign the positioning accuracy of each axis for selecting the motion components in the design stage. The error budget process for the designed laser machine is shown in Fig. 6. First, according to the laser polishing process characteristics, the targeted positioning accuracy are assigned. Based on the error contributions

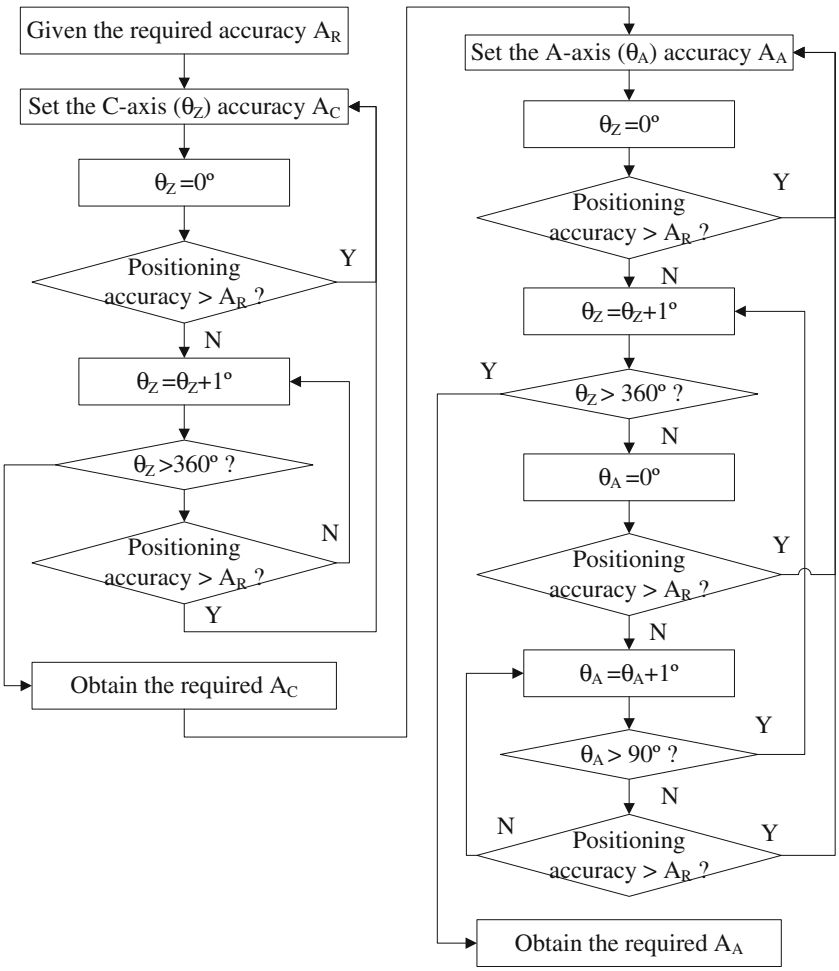

Fig. 7 Flow chart for A and C-axis accuracy identification

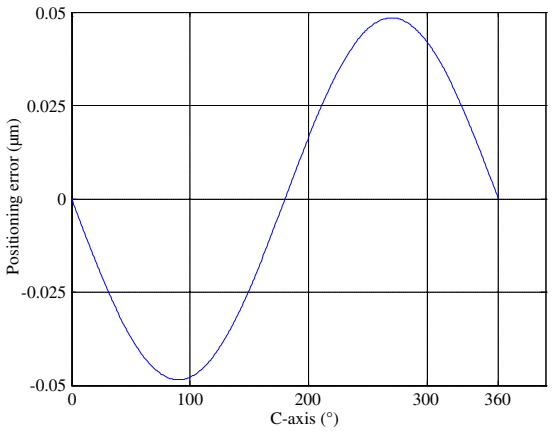

(a) X-axis positioning errors (Ac=20")

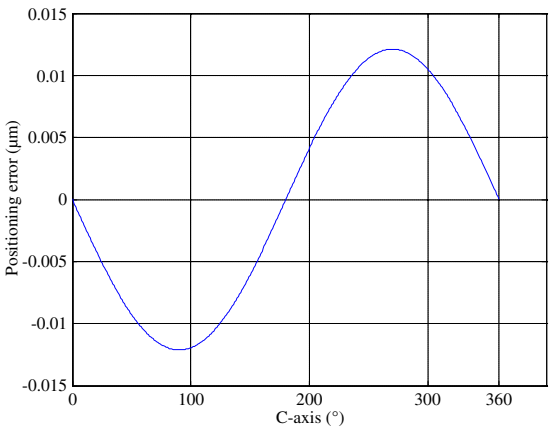

(b) X-axis positioning errors (Ac=5")

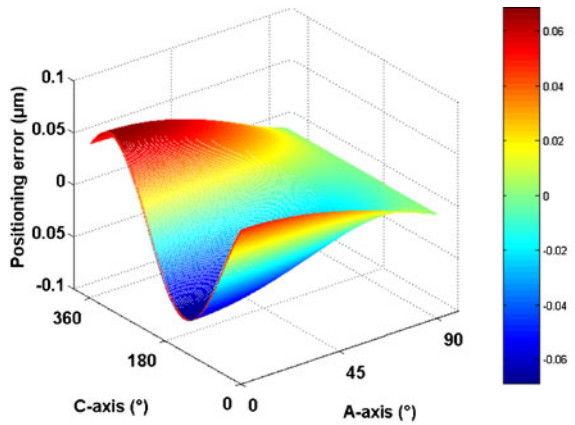

(c) Y-axis positioning errors (Ac=20", AA=0.01")

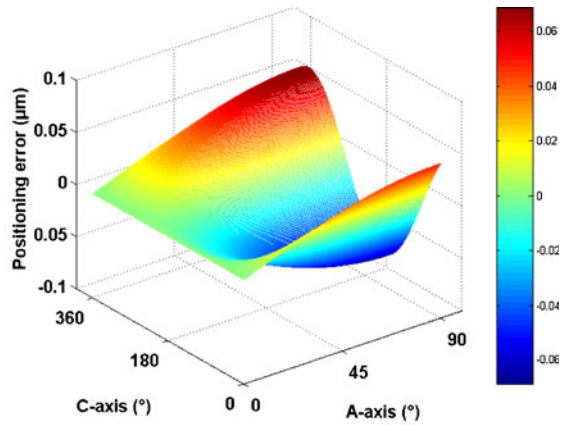

(d) Z-axis positioning errors (Ac=20", AA=0.01")

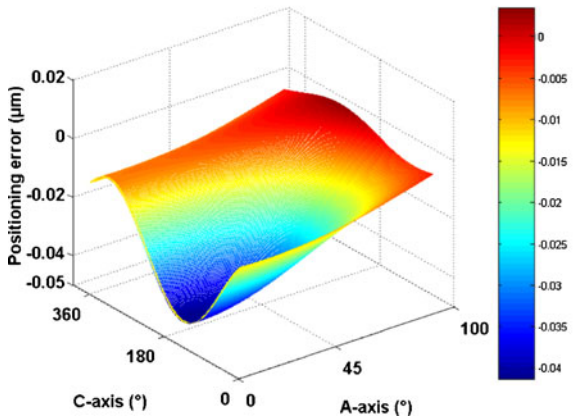

(e) Y-axis positioning errors (Ac=5", AA=1")

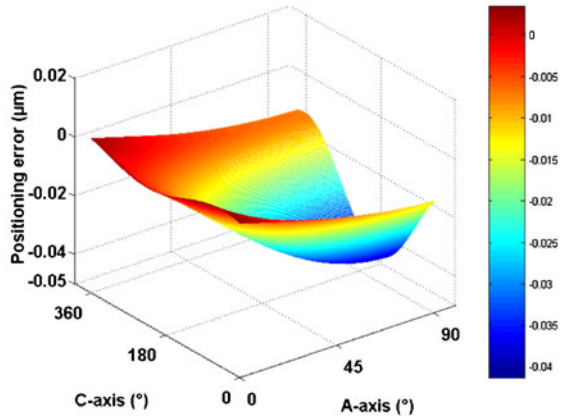

(f) Z-axis positioning errors (Ac=5", AA=1")

Fig. 8 Positioning error distribution in the workspace. **a** *X*-axis positioning errors (Ac=20″). **b** *X*-axis positioning errors (Ac=5″). **c** *Y*-axis positioning errors (Ac=20″, AA=0.01″). **d** *Z*-axis positioning errors (Ac=20″, AA=0.01″). **e** *Y*-axis positioning errors (Ac=5″, AA=1″). **f** *Z*-axis positioning errors (Ac=5″, AA=1″)

analyzed above, the accuracy needed by linear axes and rotary axes are assigned respectively. Referring to the *X*-axis positioning accuracy in Eq. 14, the positioning accuracy of C-axis can be calculated conveniently. For *A*-axis accuracy, it is decided by both *Y*- and *Z*-axis positioning accuracy. At last, by comparing the *A*-axis

accuracy needed by *Y* and *Z* axes, the smaller one is allocated to the *A*-axis.

Laser polishing techniques are used for the finish machining process [16]. It is possible to achieve the higher surface roughness than that by mechanical method. The surface roughness of Ra=0.12 μm can be achieved by ArF excimer laser polishing diamond films [17]. Therefore, it is reasonable to assign the positioning accuracy of 0.1 μm to the laser machine. To simplify the process, half of the total positioning accuracy is assigned to the linear axes and half of that is assigned to the rotary axes respectively. Namely, the positioning accuracy of 0.05 μm is needed by each linear axis and another 0.05 μm is fulfilled by the combination accuracy of both rotary axes.

By Eq. 14, the positioning accuracy needed for the two rotary axes are identified through searching the whole workspace. Figure 7 shows the flow chart for the searching process. First, the positioning accuracy for C-axis is calculated as shown in the left side in Fig. 7. Then, the required accuracy and C-axis accuracy work as the input to calculate the required *A*-axis positioning accuracy.

The positioning errors only caused by the rotary axes are shown in Fig. 8. *X*-axis positioning errors of 0.05 μm can be fulfilled when the positioning accuracy of *A*-axis is 20″ as shown in Fig. 8a. However, in order to satisfy the assigned *Y*-axis and *Z*-axis positioning accuracy, the *A*-axis positioning accuracy should be very high as shown in Fig. 8c and d. To balance the positioning accuracy of the two rotary axes, positioning accuracy of C-axis has been increased to 5″. Finally, the reasonable positioning accuracy of *A*-axis has been identified as 1″. Figure 8b, e, and f shows the final positioning accuracy all has been fulfilled in the whole workspace.

5 Conclusions

Micro tools are made of ultra or super-hard materials in order to achieve a longer tool life. Laser machining is one possible fabrication method for micro tools made of super-hard, nonconductive or very weak conductive materials. By analyzing the typical micro milling tool with comparatively complicated tool geometries, a laser tool fabrication machine with five axes has been designed based on the generative design method. Then, the kinematics of the designed laser machine has been deduced. Error budget analysis of the five-axis laser machine shows that the positioning accuracy of rotary axes has large effects on the final positioning accuracy of the workpiece. Finally, the positioning accuracy for each axis has been identified and assigned, which form a solid basis for the motion components selection on the design stage.

Acknowledgment The authors wish to express their appreciation for the financial support by the China National Science and Technology Key Project "High Quality CNC Machine Tools and Fundamental Manufacturing Equipements" with the grant number of 2009ZX04014-032 and by the Natural Science Foundation of Shandong Province, China with the grant number of ZR2011EEM010.

References

1. Jin M, Goto I, Watanabe T, Kurosawa J, Murakawa M (2007) Development of CBN ball-nosed end mill with newly designed cutting edge. J Mater Process Technol 192–193:48–54
2. Cheng X, Wang ZG, Nakamoto K, Yamazaki K (2009) Design and development of micro PCD ball end mill for micro/nano freeform machining of hard and brittle materials. J Micromech Microeng 19:115022
3. Sumiya H, Irifune T (2004) Indentation hardness of nano-polycrystalline diamond prepared from graphite by direct conversion. Diam Relat Mater 13(10):1771–1776
4. Takuya S, Ryuichi O, Hitoshi S (2010) Micro ball end mill made of nano-polycrystalline diamond. Trans Jpn Soc Mech Eng Part C 76(763):768–776
5. Puri AB, Bhattacharyya B (2003) An analysis and optimization of the geometrical inaccuracy due to wire lag phenomenon in WEDM. Int J Mach Tools Manuf 43(2):151–159
6. Klocke F, Lung D, Thomaidis D, Antonoglou G (2004) Using ultra thin electrodes to produce micro-parts with wire-EDM. J Mater Process Technol 149(1–3):579–584
7. Ho KH, Newman ST, Rahimifard S, Allen RD (2004) State of the art in wire electrical discharge machining (WEDM). Int J Mach Tools Manuf 44(12–13):1247–1259
8. Takuo O, Hiroaki O, Shoko O, Hiroyuki K, Syohei N, Mitsuru S, Hitoshi S (2009) Micromachining and surface processing of the super-hard nano-polycrystalline diamond by three types of pulsed lasers. Appl Phys A 96(4):833–842
9. Qin Y, Brockett A, Ma Y, Razali A, Zhao J, Harrison C, Pan W, Dai X, Loziak D (2010) Micro-manufacturing: research, technology outcomes and development issues. Int J Adv Manuf Technol 47(9):821–837
10. Park HW, Park YB, Liang SY (2011) Multi-procedure design optimization and analysis of mesoscale machine tools. Int J Adv Manuf Technol. doi:10.1007/s00170-011-3160-6
11. Homann BS, Thornton AC (1998) Precision machine design assistant: A constraint-based tool for the design and evaluation of precision machine tool concepts. Artif Intell Eng Des Anal Manuf 12(5):419–429
12. Zhang GP, Shi WH, Huang YM, Lei XQ (2003) Generative design of structure configurations for NC lathes. China Mech Eng 14(2):1805–1807
13. Cheng X, Wang ZG, Kobayashi S, Nakamoto K, Yamazaki K (2010) Tool fabrication system for micro/nano milling—function analysis and design of a six-axis wire EDM machine. Int J Adv Manuf Technol 46(2):179–189
14. Cheng X, Wang ZG, Kobayashi S, Nakamoto K, Yamazaki K (2009) Development of a six-axis wire electrical discharge machining machine for the fabrication of micro end mills. J Eng Manuf 223(2):121–131
15. Slocum AH (1992) Precision machine design. Prentice Hall, Dearborn, Society of Manufacturing Engineers
16. Lamikiz A, Sanchez JA, Lacalle D, Lopez LN, Delpozo D, Etayo JM (2006) Surface roughness improvement using laser-polishing techniques. Mater Sci Foru 526:217–222
17. Pimenov SM, Kononenko VV, Ralchenko VG, Konov VI, Gloor S, Luthy W, Weber HP, Khomich AV (1999) Laser polishing of diamond plates. Appl Phys A 69(1):81–88